JOURNAL OF AIRCRAFT
Vol. 46, No. 6, November–December 2009

Engineering Notes

Impulsively Started Flat Plate Flow

R. M. H. Beckwith* and H. Babinsky†
University of Cambridge,
Cambridge, CB2 1PZ England, United Kingdom

DOI: 10.2514/1.46382

Nomenclature

AR	=	semispan aspect ratio
C_L	=	coefficient of lift
C_{LSS}	=	steady-state coefficient of lift
c	=	chord length
Re	=	Reynolds number based on chord length
α	=	angle of incidence

Introduction

LIFT production associated with medium-low Reynolds number flows, specifically Reynolds numbers applicable to small bird or large insect flight, has gone largely unnoticed in the history of aerodynamic research, which has concentrated on Reynolds numbers greater than 100,000. Limited research suggests that lift coefficients observed in steady flow over airfoils in this regime are relatively low. In nature, flight in this Reynolds number regime is primarily flapping flight, dominated by unsteady mechanisms. Consequently, it is thought that micro air vehicles (MAVs) will need to exploit unsteady mechanisms and 3-D effects to generate lift. At present, the relative importance of these effects and the significance of three-dimensionality are not well understood.

The simplest approximation of flapping flight to study is the acceleration of a wing from rest, which serves to replicate either the upstroke or downstroke. This study examines forward flight, which is dominated by the downstroke (Ellington [1]). Consequently, interactions from the flowfield generated by the upstroke are ignored. Although this is a simplification to the dynamics of actual flapping, it serves as a starting point for further studies which will examine both the upstroke and the downstroke, important for maneuvers such as hovering flight. Previous studies have focused on angles normal to the flow (Lisoski [2]), whereas wings at angles of incidence have primarily been studied in 2-D, steady-state situations (Pelletier and Mueller [3]).

One of the unsteady mechanisms applicable to accelerating wings is the Wagner effect: the delay in circulation development and therefore lift production as a wing starts from rest [4]. The model predicts a gradual build in circulation which asymptotically approaches a steady-state value, reaching approximately 90% after $6c$ of travel. Because the translational phase of an insect's wingbeat will last only a few chord lengths, this delay in lift generation could be significant.

Alternative unsteady mechanisms can result in improved lift conditions. One example is dynamic stall, which is produced by a pitching aerofoil, as in a helicopter blade. A similar effect can occur on an impulsively started wing at constant angle of attack; this is referred to as delayed stall.

Because Wagner's effect [4] is predicted for angles below stall, and delayed stall is seen at angles past stall, at some point both effects may come into play. Consequently, past studies at a range of Reynolds numbers and angles of incidence have found conflicting results concerning the relative importance of these two mechanisms (Walker [5], Francis and Cohen [6], Falco et al. [7], and Dickinson and Gotz [8]). For the intermediate Re range of interest to the MAV community, the relative importance of delayed stall and the Wagner effect has not been investigated.

The current study examines a finite span flat plate with semispan $AR = 4$ accelerated from rest. This AR is relevant to hummingbirds and dragonfly wings, which generally exhibit semispan aspect ratios between three and four (derived from Ng [9]). The aim is to offer insight into what unsteady mechanisms affect lift generation on a 3-D wing at low Reynolds numbers, for angles both above and below steady-state stall, to determine if an unsteady flapping motion could offer increased lift benefits for MAV applications.

Materials and Methods

Unsteady measurements took place in the Cambridge University Engineering Department towing tank which has a 1-m-square cross section. The central section (2 m in length) is constructed of Perspex, with an additional Perspex end window to enable particle image velocimetry (PIV) imaging. The desired Reynolds number of 60,000 was achieved with a towing speed of 0.48 m/s. The plate was accelerated from rest to full speed using a linear velocity profile over a streamwise distance of 0.072 m, which is equivalent to $0.6c$.

The model consists of a flat plate of semispan = 480 mm, chord length = 120 mm, and thickness = 3 mm fabricated from aluminum. Leading and trailing edges were rounded. A clamp was designed to provide angle of attack adjustments with 5 deg increments, and one end of the wing was constrained using a 690×990 mm end plate.

A 50 N, 2-degree-of-freedom strain gauge was used to measure lift and drag forces. Data were taken at $\alpha = 5$ and 15 deg. Results were averaged from 15 separate measurements. Between each run, the water was allowed to settle for 15 min so that turbulence levels could fall to a minimum. After averaging the 15 data sets for each configuration, a moving average filter was used to remove high-frequency electrical noise from the measurements. To remove inertial forces, the tank was drained and force histories were recorded in air. The inertial signal was subtracted from all force measurements and was always less then 1% of the full-scale force signal.

A LaVision, high-speed PIV system was used for PIV imaging. Results from a laser sheet positioned at three-quarter span are presented in this Note, as pictured in Fig. 1.

Vestosint 7182 particles with a nominal diameter of 30 μm were used. Settings for analyzing the images used a multipass approach, starting with a 64×64 pixel interrogation window, and then dropping down to a 16×16 window. At each configuration, 20 separate runs provided enough data to obtain reliable averaged data sets, with 15 min settling time between each run. Further post-processing was done in Matlab to average the 20 runs; for each velocity vector point, vectors outside of 1 standard deviation from the average across the 20 runs were discarded.

For force balance measurements, standard deviations for each data point in the force history was taken across the separate, compiled runs. Uncertainty estimates were taken as the average standard

Presented as Paper 0789 at the 47th AIAA Aerospace Sciences Meeting and Exhibit, Orlando, FL, 5–8 January 2009; received 17 July 2009; revision received 25 August 2009; accepted for publication 26 August 2009.

*Ph.D. Candidate; currently Stanford University, Department of Aeronautics and Astronautics. Student Member AIAA.

†Reader in Aerodynamics, Department of Engineering, Trumpington Street. Associate Fellow AIAA.

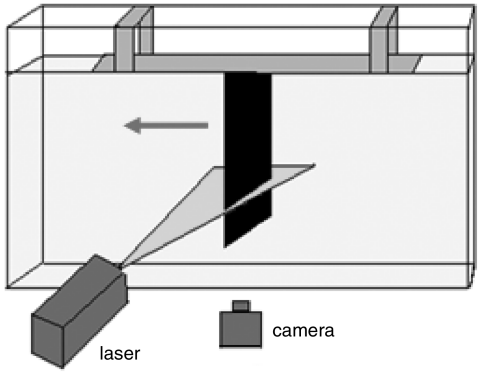

Fig. 1 Experimental setup for unsteady PIV measurements with chordwise laser sheet position.

deviation across the data set. Error bars are not included on the plot of C_L because they are essentially equal to the thickness of the plot line. Although the repeatability of the signal was very good, possible vibrations in the system introduce uncertainty about the origin of some components of the force signals. PIV is used solely to illustrate the flowfield in this note, and so errors are not quantified.

Results

Force Histories

Angle of steady-state stall was determined using wind-tunnel tests, and values of steady state C_L were determined by running the model out to $20c$ of travel and averaging the force histories over 5 s, as well as averaging force values recorded in the steady-state wind-tunnel tests [10]. Figure 2 shows the transient development of C_L for both pre- and poststall test configurations for the first $5c$ of travel. Horizontal dashed lines indicate the average steady-state value of C_L for both angles, whereas vertical dashed lines mark stages in translation illustrated further with PIV images in Fig. 3. Finally, Wagner's prediction [4] of lift development (ignoring momentum contributions and assuming that lift varies linearly with circulation as $L = \rho U\Gamma$) is plotted for each angle against chord lengths of travel.

Both force histories show a distinct peak in force around $0.6c$, which coincides exactly with the end of the acceleration period. For both angle conditions, lift drops off slightly after the $0.6c$ peak. In the case of the prestall wing, lift then gradually builds up to a steady-state value of around 0.33. This build in force looks very similar to Wagner's prediction [4], the only difference being the initial local maximum at $0.6c$.

In the case of the poststall condition ($\alpha = 15$ deg), lift builds to reach a second maximum at $3.5c$ after the initial peak and dip at $0.6c$. This is a clear case of delayed stall behavior: lift exceeds a value beyond that achieved at steady state. Lift curve shapes, including the initial peak in force, look very similar to those found by Dickinson and Gotz [8] at $Re < 1000$. In particular, they also reported that a sharp initial force peak at approximately $0.5c$ is seen in all angles of attack. In addition, for very large α, force stays at a value above steady state for the first three or four chord lengths, though smaller angles of attack do not appear to exhibit this same secondary peak in force.

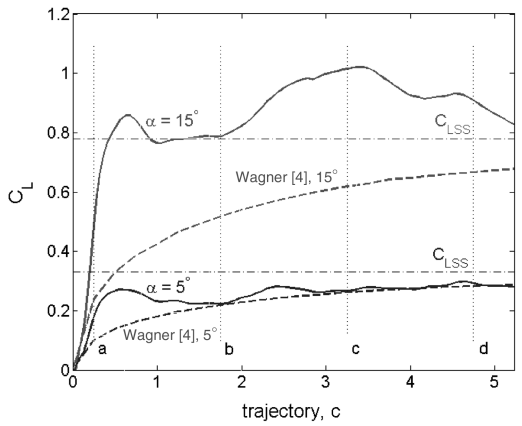

Fig. 2 C_L from compiled, filtered force balance data for $\alpha = 5$ deg and $\alpha = 15$ deg.

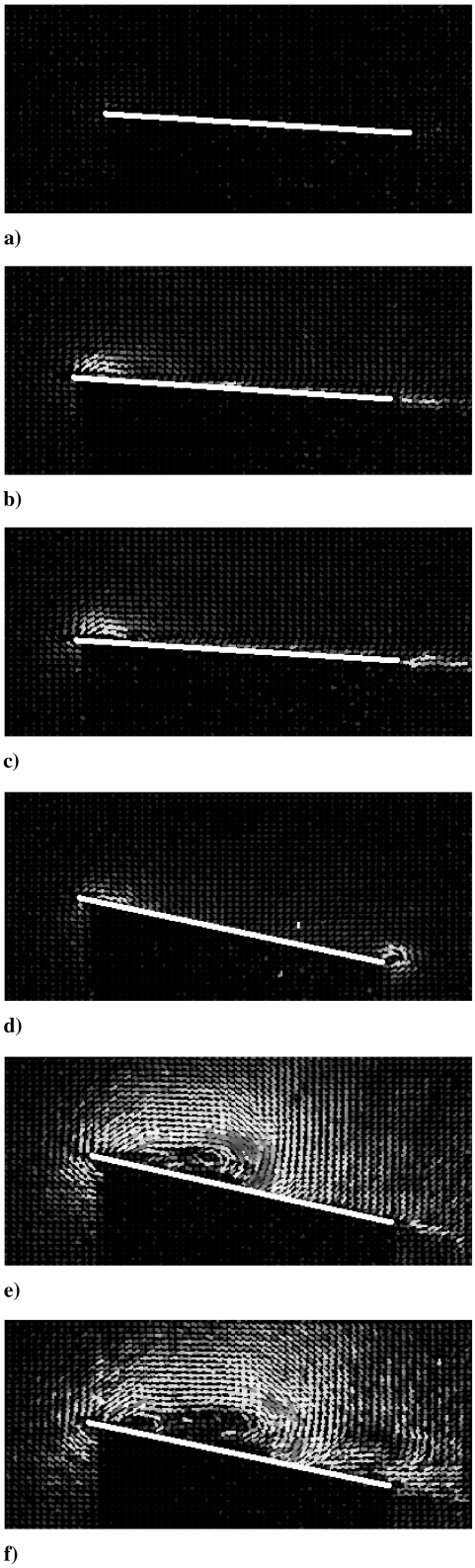

Fig. 3 Velocity vectors from PIV data taken at three-quarter span with $\alpha = 5$ deg after a) $0.25c$, b) $1.75c$, c) $3.25c$, and $\alpha = 15$ deg after d) $0.25c$, e) $1.75c$, f) $3.25c$ chord lengths of travel.

Particle Image Velocimetry

Velocity vectors obtained from averaged PIV data are shown in Fig. 3 for various stages during startup. Direction of travel in each frame is from right to left, and the dark region is in the shadow of the laser sheet on the pressure side of the wing.

After $0.25c$ of travel, the flow has begun to separate from the leading edge of the plate, forming a leading-edge vortex (LEV) for the poststall plate, and the formation of the starting vortex can be seen behind the trailing edge. Flow around the prestalled plate is slower to develop. Referring back to the force history in Fig. 2, we see that, at this point, the lift values for both plates are well below steady state. After $1.75c$ of travel, the prestall plate now shows a small, attached LEV, while the flow around the stalled plate appears to have completely separated until halfway along the chord where it reattaches. At this point, the lift coefficient on the stalled plate is basically equal to the steady-state value. As the plate continues to translate through $3.25c$ of travel, the region of separation slowly extends further down the chord of the plate for the poststall plate as the lift coefficient exceeds steady-state values, while the prestall condition continues to exhibit a stable LEV with an attached flowfield and a lift value below steady state. The force histories and the PIV data observed for the two angles suggest that different mechanisms are important depending on the angle of attack of the plate.

Because the translational phase in a typical insect wingbeat will only last between two and four chord lengths (Dickinson and Gotz [8]), this transient period in force production is very significant. These results show that translating a wing at angles that would produce stalled conditions in steady state can actually benefit lift production on the time scales seen in flapping flight, whereas an angle that exhibits attached flow in a steady regime would be detrimental to lift production.

Conclusions

An experimental study was conducted of a flat plate wing impulsively started from rest using PIV flow characterization and force balance histories. Transient force balance data indicate that, while the prestall plate shows a gradual build in lift force similar to Wagner's prediction [4], the lift on the poststall plate rises more quickly to levels above steady state, a clear example of delayed stall. Force curves are similar in shape to those seen by Dickinson and Gotz [8] at $Re < 1000$, including the initial sharp transient peak at around $0.5c$.

The characterization of the flowfield and lift production capabilities of a flat plate wing accelerated from rest in both pre- and poststall configurations show that, at this medium-low Reynolds number applicable to large insects and MAVs, in the first $5c$ of translation, delayed stall works to increase lift past steady-state capabilities for an angle of attack above steady-state stall. However, at angles of attack below steady-state stall, the Wagner effect [4] is evident, which reduces lift capabilities. It is possible that the Wagner effect is always present, but at angles above stall is dominated by other unsteady effects. In addition, the initial peak in force histories may be the result of the LEV reaching maximum strength before detaching.

Acknowledgments

This work was supported by U.S. Air Force Office of Scientific Research grant FA8655-07-1-3082. The authors would also like to thank M. Ol and G. Abate as well as A. R. Jones for valuable discussion and comments.

References

[1] Ellington, C. P., "The Aerodynamics of Hovering Insect Flight III: Kinematics," *Philosophical Transactions of the Royal Society of London, Series B: Biological Sciences*, Vol. 305, No. 1122, 1984, pp. 41–78.

[2] Lisoski, D. L. A., "Nominally Two-Dimensional Flow About a Normal Flat Plate," Ph.D. Thesis, California Inst. of Technology, Pasadena, CA, 1993.

[3] Pelletier, A., and Mueller, T., "Low Reynolds Number Aerodynamics of Low-Aspect Ratio Thin/Flat/Cambered-Plate Wings," *Journal of Aircraft*, Vol. 37, No. 5, 2000, pp. 825–832. doi:10.2514/2.2676

[4] Wagner, H., "Uber die enstehung des dynamischen auftriebes von tragflugeln," *Zeitschrift für Angewandte Mathematik und Mechanik*, Vol. 5, 1925, pp. 17–35.

[5] Walker, P. B., "Experiments on the Growth of Circulation About a Wing," Aeronautical Research Comm. Technical Rept. 1402, 1931.

[6] Francis, R. H., and Cohen, J., "The Flow near a Wing Which Starts Suddenly from Rest and then Stalls," Aeronautical Research Comm., Memo No. 1561, 1933.

[7] Falco, R. E., Chu, C. C., Hetherington, M. H., and Gendrich, C. P., "The Circulation of an Airfoil Starting Vortex Obtained from Instantaneous Vorticity Measurements over an Area," *First AIAA, ASME, SIAM and APS, National Fluid Dynamics Congress*, AIAA, Washington, D.C., July 1988, pp. 1048–1054.

[8] Dickinson, M. H., and Gotz, K. G., "Unsteady Aerodynamic Performance of Model Wings at Low Reynolds Numbers," *Journal of Experimental Biology*, Vol. 192, 1993, pp. 179–206.

[9] Ng, S., "Low Speed Aerodynamics of Insect Flight," Ph.D. First Year Rept., University of Cambridge, Cambridge, England, U.K., 2008.

[10] Beckwith, R. M. H., and Babinsky, H., "Impulsively Started Flat Plate Wing 2009-0789," *47th AIAA Aerospace Sciences Meeting and Exhibit* [CD-ROM], AIAA, Reston, VA, 2009.